search for foraging sites while facing in the direction in which they leave the hive, whereas bees learning how to return home face towards the entrance.

In conclusion, the bees we studied tended to face south. They did this both while learning about the immediate vicinity of a feeder and when returning to it. In this way, retinotopic and compass-based coordinates are automatically kept in register. Two findings suggest that a standard viewing direction is important in handling retintopic memories. First, the preferred orientation shifts away from south when the defining landmark lies to the north of the feeder and so cannot be seen by a bee facing south; and second, bees hold to the shifted orientation induced by an imposed magnetic field after the magnets have been removed. Bees can thus orientate by means of their visual surroundings using memories stored while facing magnetic south. □

Received 12 October 1993; accepted 18 January 1994.

1. Wehner, R. in *Handbook of Sensory Physiology* vol. VII/6C (ed. Autrum, H. J.) 287–616 (Springer, Berlin, 1981).
2. Collett, T. S. *Phil. Trans. R. Soc. Lond.* B**337,** 295–303 (1992).
3. Wehner, R. *J. comp. Physiol.* **77,** 256–277 (1972).
4. Dill, M., Wolf, R. & Heisenberg, M. *Nature* **365,** 751–753 (1993).
5. Lindauer, M. *Cold Spring Harb. Symp. quant. Biol.* **25,** 371–377 (1960).
6. Batschelet, E. *Circular Statistics in Biology* (Academic, London, 1981).
7. Opfinger, E. *Z. vergl. Physiol.* **15,** 431–487 (1931).
8. Couvillon, P. A. & Bitterman, M. E. *J. Insect Behav.* **5,** 123–129 (1992).
9. Lehrer, M. *J. comp. Physiol.* A**172,** 549–563 (1993).
10. Tinbergen, N. *Z. vergl. Physiol.* **16,** 305–335 (1992).
11. Zeil, J. *J. comp. Physiol.* A**172,** 189–205 (1993).
12. Zeil, J. *J. comp. Physiol.* A**172,** 207–222 (1993).
13. von Frisch, K. *The Dance Language and Orientation of Bees* (Belknap, Cambridge, 1967).
14. Wehner, R. & Rossel, S. in *Experimental Behavioral Ecology and Sociobiology* (eds Hölldobler, B. & Lindauer, M.) 11–53 (Sinauer, Sunderland, 1985).
15. Lindauer, M. & Martin, H. *Z. vergl. Physiol.* **60,** 219–243 (1968).
16. Martin, H. & Lindauer, M. *J. comp. Physiol.* **122,** 145–187 (1977).
17. Gould, J. L., Kirschvink, J. L. & Deffeyes, K. S. *Science* **201,** 1026–1028 (1978).
18. Walker, M. M. & Bitterman, M. E. *J. exp. Biol.* **145,** 489–494 (1989).
19. Kirschvink, J. L. & Kobayashi-Kirschvink, A. *Am. Zool.* **31,** suppl. (1), 169–185 (1991).
20. Schmitt, D. E. & Esch, H. E. *Naturwissenschaften* **80,** 41–43 (1993).
21. Vollbehr, J. *Zool. Jb. Physiol.* **79,** 33–69 (1975).

ACKNOWLEDGEMENTS. We thank E. Godwin for the loan of bees, and M. Land and D. Osorio for scrutinizing the typescript. Financial support came from SERC.

Turning of nerve growth cones induced by neurotransmitters

James Q. Zheng, Mark Felder, John A. Connor* & Mu-ming Poo†

Department of Biological Sciences, Columbia University, New York, New York 10027, USA
* Roche Institute of Molecular Biology, Roche Research Center, Nutley, New Jersey 07110, USA

PATHFINDING by growing nerve processes in the developing nervous system depends on the turning response of the growing tip, the growth cone, to extracellular guidance cues[1–4]. There is evidence *in vivo* and in cell culture that some growth cones exhibit chemotropic behaviour[5–12], but the identity of endogenous chemoattractants remains elusive. Neurotransmitters appear early in the developing embryo and may have morphogenic roles in development[13,14]. In cell culture a number of neurotransmitters were found to induce growth inhibition or retraction of neurites[15–19]. Here we report positive turning responses of the nerve growth cone in a defined extracellular gradient of the neurotransmitter acetylcholine (ACh). The growth cone response depends on the activation of neuronal nicotinic ACh receptors, requires the presence of extracellular Ca^{2+}, and appears to be mediated by Ca^{2+}–calmodulin-dependent protein kinase II. Fluorescence imaging of cytosolic Ca^{2+} concentration ($[Ca^{2+}]_i$) at the growth cone showed a small but significant evaluation of $[Ca^{2+}]_i$ within minutes of the onset of ACh application and before the turning of the growth cone. These findings suggest that neurotransmitters may serve as specific chemoattractants for growth cone guidance and that cytosolic Ca^{2+} may act as a second messenger in the cytoplasm of the growth cone to initiate the turning response.

Isolated embryonic spinal neurons in *Xenopus* cell cultures were used. Microscopic gradients of ACh molecules near the growth cone were established by repetitive pulse application of picolitres of concentrated solution from a micropipette[20]. The profile of chemical gradients produced by this method was monitored quantitatively using a fluorescent dye, 5-carboxyfluorescein. Under repetitive pulse application, a relatively stable gradient of chemicals can be quickly established by diffusion over a distance of a few hundred micrometres (Fig. 1). Quantitative measurement indicates that at a distance of 100 μm from the source of the chemical, a gradient of up to ~12% can be

† To whom the correspondence should be addressed.

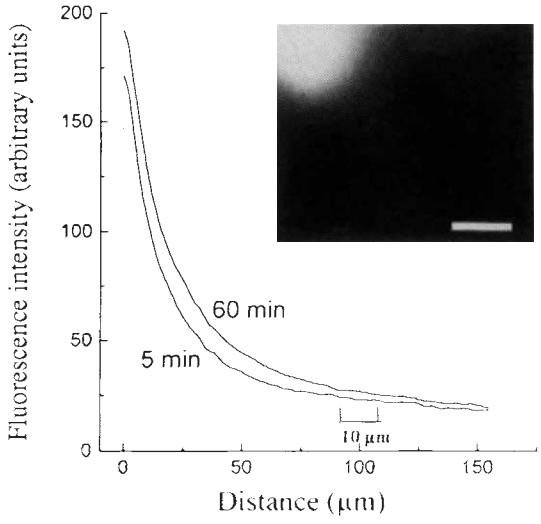

FIG. 1 Gradient of chemicals created by repetitive pulsatile ejection from a micropipette. 5-carboxyfluorescein was used to demonstrate the gradient. The fluorescence intensity surrounding the source pipette was measured 5 and 60 min after the onset of repetitive pulses. The steepness of the gradient at 100 μm (across 10 μm distance, as marked) was estimated to be 4 and 12%, respectively, at 5 min and 60 min. A fluorescent image of the gradient (at 60 min) is shown in the inset (scale bar, 50 μm).
METHODS. Micropipette (tip opening, 1 μm) was filled with 1 mM 5-carboxyfluorescein dissolved in culture medium, and was connected to an electrically gated pressure application system (Picospritzer, General Valve Co.). Positive pressure of 3 psi was applied to the pipette with a frequency of 2 Hz and a duration of 10 ms using a pulse generator (SD9, Grass Co.). The average volume of the ejected solution per pulse was estimated to be in the range 0.3–0.7 pl (ref. 20). Pulsatile ejection of 5-carboxyfluorescein and fluorescence microscopy were performed on an inverted microscope (Axiovert 35, Zeiss) equipped with fluorescence attachments and a ×20 objective. After the onset of pulsatile ejection, fluorescent images were collected by a cooled CCD (charge coupled device) camera (Star I, Photometrics, Tucson, AZ), which has a dynamic range of up to 4096 gray levels in intensity. The intensity profile of the fluorescent gradient was then measured pixel by pixel over a distance of a few hundred microns. The background reading before application of fluorescence dye was subtracted from all intensity measurements.

TABLE 1 Response of *Xenopus* nerve growth cones in ACh gradients

[ACh] in pipette	Chemicals in bath	Turning angle (deg)*	Net neurite extension (μm)*	Turning responses (%)† +	0	−	Number of cells examined
0 mM	None	−5.1 ± 4.6	24.9 ± 2.1	33	33	33	21
10 mM	None	−1.2 ± 5.5	30.8 ± 3.6	35	35	30	23
30 mM	None	9.4 ± 5.4**	23.0 ± 2.7	62	19	19	21
100 mM	None	21.0 ± 3.8**	25.2 ± 2.9	71	17	12	41
100 mM	D-Tubocurarine (100 μM)	−2.9 ± 5.6	25.3 ± 2.6	41	16	43	37
100 mM	Atropine (1 μM)	10.1 ± 5.2**	36.9 ± 4.0**	50	15	35	20
100 mM	Calcium-free‡	−7.7 ± 4.6	84.2 ± 3.8**	17	22	61	18
100 mM	KN62 (2.5 μM)§	−8.0 ± 6.1	24.3 ± 3.5	37	21	42	24

* Pulses of ACh were pressure-ejected into the bath through a micropipette at a position 100 μm away from the growth cone and an angle of 45° with respect to the direction of neurite extension. The turning angles with respect to the original direction of growth were determined by a straight line connecting the position of the growth cone at 2 h after the onset of ACh application to that at the onset. The length of neurite extension was measured for the entire trajectory of the path of extension during the 2-h period (Fig. 2e, *f*). Values represent mean ±s.e., Values marked with double asterisks were different from the control (first row, $P < 0.05$, *t*-test). The value of the turning angle for the atropine experiment was not significantly different from that of ACh (100 mM) or ACh (30 mM) with $P > 0.05$.

† Growth cone turning responses were scored as follows: plus sign refers to the percentage of cells showing positive turning towards the ACh source (turning angle >5°); 'zero' refers to cells showing no turning (|turning angle| ≤5°); and minus sign refers to cells turning away from the ACh source (turning angle < −5°).

‡ Calcium-free solution: 115 mM NaCl, 2.6 mM KCl, 5 mM $MgCl_2$, 2 mM EGTA, 10 mM HEPES, pH 7.4.

§ KN62, which is 1 − [*N*, *O*-bis(5-isoquinolinesulphonyl)-*N*-methyl-L-tyrosyl]-4-phenylpiperazine (Calbiochem), was added to the bath solution 20 min before ACh application and was present through the experiment.

established across a distance of 10 μm, or approximately the width of a growth cone, a result consistent with a previous theoretical estimate[20]. In this study, the source of ACh was placed 100 μm from the centre of the growth cone and at an angle of 45° from the direction of neurite extension. With an ACh concentration of 100 mM in the source pipette (tip opening, 1 μm) and standard pulse parameters (frequency, 2 Hz; duration, 10 ms; pulse pressure, 3 psi), consistent turning of the growth cone towards the pipette tip was observed within 2 hours of the onset of ACh application (Fig. 2*a*, *b*). No turning was observed when D-turbocurarine, a nicotinic antagonist, was present in the bath medium (Fig. 2*c*, *d*). To illustrate better the ACh-induced turning response, the path of neurite extension of a number of cells during the 2-h period of ACh application in

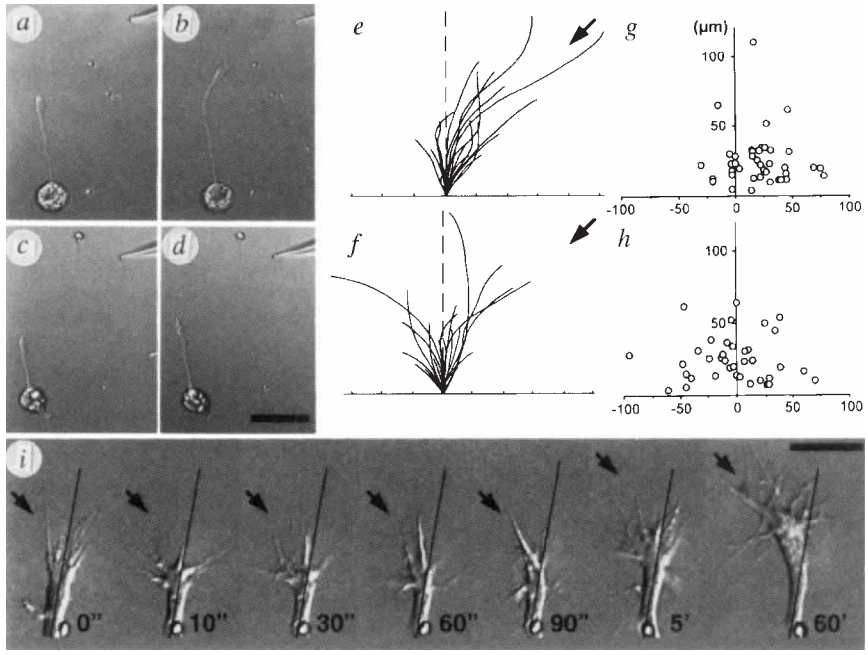

FIG. 2 Turning response of *Xenopus* spinal neurons in the presence of ACh gradient. The gradient was created by pulsatile ejection of picolitres of 100 mM ACh solution through a micropipette. *a–d*, Representative DIC images at the onset and 2-h after the application of ACh gradient in the absence (*a*, *b*) and presence (*c*, *d*) of 0.1 mM D-tubocurarine. Scale in *d* is 50 μm. *e*, *f*, Composite drawings of the path of neurite extension during a 2-h period for a population of neurons in the absence (*e*) and presence (*f*) of D-tubocurarine (0.1 mM). For clarity, only part of the data (all cases examined during the most recent 8-month period) were illustrated for each drawing. The origin represents the position of the centre of the growth cone palm at the onset of the ACh application. The original direction of neurite extension, as defined by the last 20-μm segment of the neurite at the onset of the ACh application, was aligned with the vertical dashed line. The line depicts the trajectory of the neurite after a 2-h exposure to the ACh gradient. Arrows indicate the direction of the ACh gradient. Scale, 10 μm. *g*, *h*, Scatter plots of all data corresponding to experiments illustrated in *a–f*. Each point represents the result of the turning angle and the net neurite extension, of one 2-h ACh gradient experiment in the absence (*g*) and presence (*h*) of D-tubocurarine (abscissa in degrees, ordinate in μm). *i*, DIC images of a growth cone subjected to the ACh gradient before and at various times after the onset of the ACh gradient. Arrows indicate the direction of the ACh pipette. Lines indicate the original direction of neurite extension. Note the asymmetric filopodial distribution within the first minute after the onset of ACh application, and the eventual turning of the growth cone at 60 min. Scale, 20 μm.

METHODS. Cultures were prepared according to procedures reported previously[38–40]. Briefly, the neural tube tissue from 1-day-old embryo was dissociated in Ca^{2+}- and Mg^{2+}-free Ringer's solution supplemented with EDTA, plated on clean glass coverslips, and incubated at room temperature (20–22 °C) for 6 to 10 h before the experiments. The culture medium consists of 50% (v/v) of Leibovitz medium (GIBCO), 2% (v/v) of fetal calf serum (GIBCO), and 48% (v/v) of Ringer's solution (115 mM NaCl, 2 mM $CaCl_2$, 2.5 mM KCl and 10 mM HEPES, pH 7.3). The ACh gradient was produced with a protocol similar to that described in Fig. 1. The micropipette containing 100 mM ACh chloride was positioned at a distance of 100 μm from the centre of the growth cone and at an angle of 45° from the direction of neurite extension. ACh was ejected at a frequency of 2 Hz and a pulse duration of 10 ms. The microscopic images were obtained with a 20 × objective, collected by a CCD camera (Fig. 1), processed with an image processor (Image Technology Model 151), and stored on an optical memory disk recorder (Panasonic TQ 2026F).

the absence and presence of D-tubocurarine in the bath is presented as composite drawings (Fig. 2*e*, *f*, respectively). The angle of growth cone turning was defined by the angle between the original direction of extension and the line connecting the position of the growth cone at the onset and at 2 h after the onset of the ACh application. Figure 2*g*, *h* depicts the data on the turning angle and the length of extension for all growth cones examined in the experiments shown in Fig. 2*a*–*f*. Table 1 summarizes quantitative measurements of the angle of turning, the length of neurite extension, and the percentage of cells showing turning responses under various experimental conditions. Significant turning was also observed when the ACh concentra-

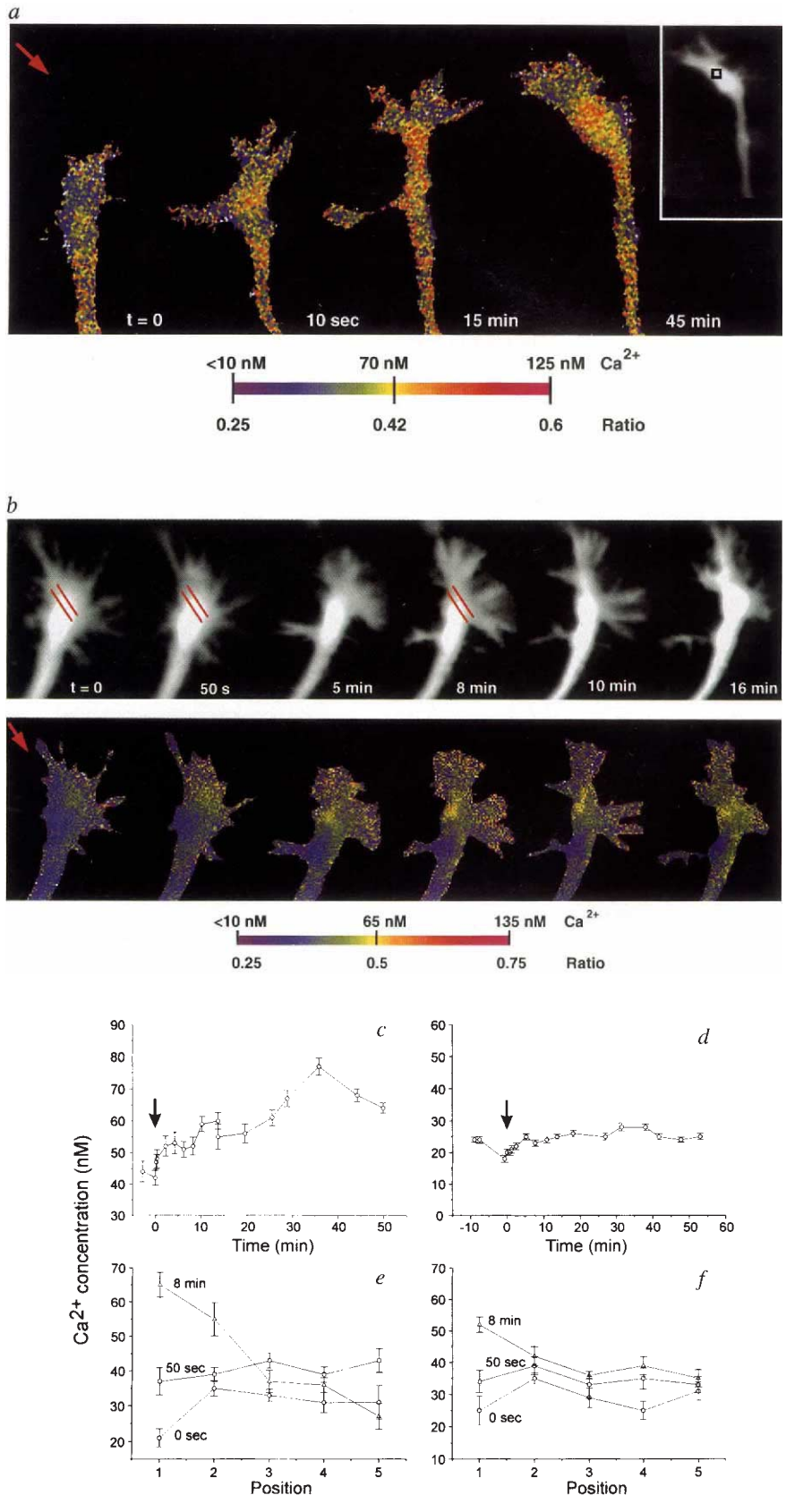

FIG. 3 Fura-2 imaging of $[Ca^{2+}]_i$ in the growth cone during ACh-induced turning. *a*, A growth cone showing a Ca^{2+} increase after the onset of ACh application. The level of $[Ca^{2+}]_i$ is shown in pseudocolours with the corresponding Ca^{2+} concentration and fluorescence ratio at 340 and 380 nm depicted by the colour bar. The ACh gradient was applied in the same way as for Fig. 2. The source of ACh was located 45° from the direction of neurite extension in the upper-left corner (red arrow). Fluorescence image at 380 nm excitation is shown in the inset on the right; black box shows the point of $[Ca^{2+}]_i$ measurement. *b*, Another growth cone exhibiting a gradient of Ca^{2+} during the first few minutes after application of the ACh gradient. Top panel shows a time-lapse sequence of fluorescence images of the growth cone at 380 nm excitation, and the bottom panel shows the corresponding pseudocolour Ca^{2+} images. Note the increase in the Ca^{2+} level on the side of the growth cone facing the source of ACh. Red lines depict the positions of quantitative Ca^{2+} measurements illustrated in *e* and *f*. *c*, $[Ca^{2+}]_i$ levels at different times after the onset of the ACh application at the centre of the growth cone shown in *a*. The size of the measurement box was 5 × 5 pixels and the data shown are mean ± s.e. Arrow indicates the onset of ACh application. *d*, Similar measurements as *c* for another growth cone in the presence of D-tubocurarine (0.1 mM) in the bath. *e* and *f*, $[Ca^{2+}]_i$ was measured along the direction of the gradient at three different times ($t = 0$, 50 s and 8 min) after the onset of ACh application. Five measurements were made along the red line shown in *b* from the upper left to the lower right (corresponding to values at 1 to 5). Data in *e* and *f* are for measurements along the left and right red lines, respectively. The size of the measurement box was 3 × 3 pixels and the data shown are mean ± s.e.

METHODS. For fluorescence imaging of $[Ca^{2+}]_i$, *Xenopus* cultures plated on glass coverslips were incubated in culture medium containing 3–6 μM Fura-2-AM for 30 min at room temperature. They were then carefully rinsed and mounted on the stage of an inverted microscope, equipped with a cooled CCD-based imaging system[34]. To limit excitation beam intensity, light from a 100W Hg bulb was collected using a standard glass condenser (instead of quartz) and then passed through a 1.0 neutral density filter. Excitation wavelengths were 340/380 nm, with an exposure time of 100 ms at each wavelength. To check for de-esterification and activation of the Fura-2, ionomycin (2 μM) was added to the culture medium at the end of experiments. Ratio values within 15% of the *in vitro* R_{max} (340/380 excited fluorescence) were routinely observed, which was indicative of nearly complete de-esterification.

tion in the ejection pipette was 30 mM. Based on a previous analysis[20], we estimated the ACh concentration at the growth cone to be about 1,000-fold lower, or 30 μM for the latter condition. The presence of D-tubocurarine (100 μM) abolished the turning response without significantly affecting the rate of extension. In contrast, significant turning was still observed when a muscarinic antagonist, atropine (1 μM), was present in the culture medium. These findings suggest that the turning response of the growth cone in the presence of an ACh gradient was a result of the activation of nicotinic ACh channels in the neuronal membrane. Finally, neurite retraction or growth inhibition was consistently observed when glutamate (100 mM) was used instead of ACh in the ejection pipette, a result consistent with a previous report[18].

There was substantial variability in the ACh-induced turning response of growth cones (Fig. 2*e*). This may be due in part to the heterogeneity of neuronal types in this culture, although previous studies have shown that the majority of these neurons are cholinergic in nature and are capable of forming functional synapses with co-cultured muscle cells[21,22]. It is also possible that all growth cones are affected by the ACh gradient, but random directional biases of the growth cones before the experiment may have affected the turning response to varying degrees in different cells. Such individual variability and the overall response were also observed previously for the turning response of these neurons induced by focal electric fields[23] and by gradients of dibutyryl-cAMP[20].

The turning of the growth cone in the presence of the ACh gradient provides an opportunity to examine the cellular responses underlying the turning behaviour, particularly events that precede turning. High-resolution differential interference contrast (DIC) optics were used to monitor the filopodial activity of the growth cone after the onset of ACh application. As shown in Fig. 2*i*, more filopodia appeared on the side of the growth cone facing the gradient within minutes of the onset of ACh application but before the bending of the main trunk of the growth cone. This suggests that the initial response of the growth cone in an ACh gradient was a preferential filopodial extension towards the source of ACh.

Cytosolic Ca^{2+} levels modulate the extension and motility of growth cones in a variety of neurons[24–27], and ACh triggers Ca^{2+} influx through nicotinic ACh receptors[28,29]. Extracellular focal application of electric fields at the growth cone resulted in a local elevation of $[Ca^{2+}]_i$ and increased the number of filopodial protrusions[26,27]. The possibility that Ca^{2+} influx is responsible for initiating the ACh-induced turning response of the growth cone was tested by experiments using Ca^{2+}-free medium. Consistent with a previous report[30], the rate of neurite extension was markedly increased when the culture medium was substituted with Ca^{2+}-free Ringer's saline supplemented with 2 mM EGTA and 5 mM Mg^{2+}. However, this Ca^{2+}-free medium did not deplete cytoplasmic Ca^{2+} levels (J.Z., M-m.P. and J.A.C., manuscript in preparation). When an ACh gradient similar to those used for Fig. 2 was established near the growth cone in the Ca^{2+}-free medium, the turning response of the growth cone was abolished (Table 1), suggesting that Ca^{2+} influx is required. Furthermore, when KN62, a specific inhibitor[31,32] of calmodulin-dependent protein kinase II (CaM kinase II), was added to the culture medium before and during application of the ACh gradient, the turning response was completely inhibited whereas the neurite extension was not affected (Table 1). Taken together with the results of experiments using channel antagonists, these findings suggest that extracellular ACh gradients act by activating nicotinic ACh channels, and that the resultant Ca^{2+} influx and subsequent activation of CaM kinase II are responsible for initiating the turning response.

Growth cone Ca^{2+} levels were monitored by ratio imaging of Fura-2 (refs 33–35). We observed a small but detectable elevation of $[Ca^{2+}]_i$ after the onset of ACh application (Fig. 3). The elevation was mainly restricted to the growth cone and occurred before detectable turning of the growth cone. A rapid increase in $[Ca^{2+}]_i$ at the growth cone within seconds following the onset of the ACh gradient was observed in many cases (Fig. 3*a*, *c*). In the absence of ACh in the ejection pipette or in the presence of D-tubocurarine in the bath, Ca^{2+} level was stable within ~5 nM (Fig. 3*d*). We therefore consider a $[Ca^{2+}]_i$ rise of greater than 10 nM as significant. Within 30 min after the onset of the ACh gradient (100 mM in the pipette), a significant $[Ca^{2+}]_i$ increase at the centre of the growth cone was observed in 17 out of 53 growth cones examined. This may be an underestimate of the number of the neurons that actually exhibited $[Ca^{2+}]_i$ increases because of the small magnitude or the possible transient nature of $[Ca^{2+}]_i$ increase in these growth cones. The mean $[Ca^{2+}]_i$ increase at the centre of the growth cone for all cases showing significant $[Ca^{2+}]_i$ elevation (measured with box size of 5×5 pixels) was 18 ± 3 nM (s.e., $n = 17$). When there was no ACh in the ejection medium ($n = 3$) or when D-tubocurarine was added in the bath ($n = 7$), there was no increase of $[Ca^{2+}]_i$ (Fig. 3*d*). Furthermore, a gradient of $[Ca^{2+}]_i$ at various regions of the growth cone along the direction of the ACh gradient was found in a few relatively large growth cones (Fig. 3*b*, *e*, *f*). Such a cytoplasmic $[Ca^{2+}]_i$ gradient may be responsible for initiating the turning response. We noted, however, that in these imaging experiments the frequency of ACh-induced turning responses (defined as turning angle $>5°$) at the end of a 2-h period (7 out of 20 cases) was much lower than that observed without fluorescence imaging (29 out of 41 cases). Fura-2 loading and fluorescence imaging may have produced cytotoxic effects and $[Ca^{2+}]_i$ gradients may have been smeared by an indicator 'shuttling' effect. Our findings on the $[Ca^{2+}]_i$ elevation before the growth cone turning are consistent with the role of $[Ca^{2+}]_i$ in regulating growth cone motility[25–27]. A small increase in $[Ca^{2+}]_i$ is appropriate and required for the extension and turning response of the growth cone. Higher elevation of $[Ca^{2+}]_i$ is likely to induce growth inhibition or neurite retraction. Indeed, increases in $[Ca^{2+}]_i$ greater than 300 nM were observed following application of a glutamate gradient (data not shown), which induced retraction of these *Xenopus* neurites. Previous studies on snail and hippocampal neurons have also demonstrated a correlation between growth inhibition and a marked elevation of $[Ca^{2+}]_i$ after application of neurotransmitters or electrical stimulation[25,26,36,37].

In conclusion, our results indicate that a gradient of ACh may produce a positive chemotropic effect on nerve growth. It is possible that localized secretion of neurotransmitter by the target tissue or other neurons in the embryo may influence the direction of neurite growth. Whether appropriate temporal and spatial patterns of extracellular neurotransmitter exist within the developing embryo and play a role in the pathfinding of nerve processes remains to be investigated. As a gradient of $[Ca^{2+}]_i$ elevation may initiate the growth cone turning response, other diffusible or substrate-bound factors that result in an asymmetric Ca^{2+} influx at the growth cone are all potential chemoattractants. □

Received 26 July; accepted 24 December 1993.

1. Purves, D. & Lichtman, J. W. *Principles of Neural Development* (Sinauer, Sunderland, MA, 1985).
2. Letourneau, P. in *Molecular Bases of Neural Development* (eds Edelman, G. M., Gall, W. E. & Cowan, W. M.) 269–293 (Wiley, New York, 1985).
3. Landmesser, L. *Trends Neurosci.* **9,** 489–491 (1986).
4. Bray, D. & Hollenbeck, P. J. *A. Rev. Cell Biol.* **4,** 43–61 (1988).
5. Letourneau, P. C. *Devel Biol.* **66,** 183–196 (1978).
6. Gunderson, R. & Barret, J. N. *Science* **206,** 1079–1080 (1979).
7. Lumsden, A. G. S. & Davis, A. M. *Nature* **306,** 786–788 (1983).
8. Tessier-Lavigne, M., Placzek, M., Lumsden, A. G. S., Dodd, J. & Jessel, T. M. *Nature* **336,** 775–778 (1988).
9. Menesini-Chen, M. G., Chen, J. S. & Levi-Montalcini, R. *Arch. Ital. Biol.* **116,** 53–84 (1978).
10. Jeffner, C. D., Lumsden, A. G. S. & O'Leary, D. D. M. *Science* **247,** 217–220 (1990).
11. McCraig, C. D. *J. Physiol.* **375,** 39–54 (1986).
12. Yaginuma, H. & Oppenheim, R. W. *J. Neurosci.* **11,** 2598–2613 (1991).
13. Buznikov, G. A., Chudakova, I. V., Berysheva, L. V. & Vyazmina, N. M. *J. Embryol. exp. Morph.* **20,** 119–128 (1968).
14. Lauder, J. M. *Prog. Brain Res.* **73,** 365–387 (1988).
15. Haydon, P. G., McCobb, D. P. & Kater, S. B. *Science* **226,** 561–564 (1984).

16. McCobb, D. P., Haydon, P. G. & Kater, S. B. *J. Neurosci. Res.* **19,** 19–26 (1988).
17. Lankford, K. L., DeMello, F. G. & Klein, W. L. *Proc. natn. Acad. Sci. U.S.A.* **85,** 2839–2843 (1988).
18. Mattson, M. P., Dou, P. & Kater, S. B. *J. Neurosci.* **8,** 2087–2100 (1988).
19. Lipton, S. A., Forsch, M. P., Pillips, M. D., Tauck, D. L. & Aizenmann, E. *Science* **239,** 1293–1296 (1988).
20. Lohof, A. M., Quillan, M., Dan, Y. & Poo, M-m. *J. Neurosci.* **12,** 1253–1261 (1992).
21. Xie, Z. P. & Poo, M-m. *Proc. natn. Acad. Sci. U.S.A.* **83,** 7069–7073 (1986).
22. Evers, J., Laser, M., Sun, Y., Xie, Z. P. & Poo, M-m. *J. Neurosci.* **9,** 1523–1539 (1989).
23. Patel, N. & Poo, M-m. *J. Neurosci.* **4,** 2939–2947 (1984).
24. Mattson, M. P. & Kater, S. B. *J. Neurosci.* **7,** 4034–4043 (1987).
25. Rehder, V. & Kater, S. B. *J. Neurosci.* **12,** 3175–3186 (1992).
26. Davenport, R. W. & Kater, S. B. *Neuron* **9,** 405–416 (1992).
27. Bedlack, R. S. Jr, Wei, M.-d. & Loew, L. M. *Neuron* **9,** 393–403 (1992).
28. Vernino, S., Amador, M., Luetje, C. W., Patrick J. & Dani, J. A. *Neuron* **8,** 127–134 (1992).
29. Vijayaraghavan, S., Pugh, P. C., Zhang, Z. W., Rathouz, M. M. & Berg, D. K. *Neuron* **8,** 353–362 (1992).
30. Bixby, J. L. & Spitzer, N. C. *Devl Biol.* **106,** 89–96 (1984).
31. Tokumitsu, H. *et al. J. biol. Chem.* **265,** 4315–4320 (1990).
32. Ito, I., Hidaka, H. & Sugiyama,H. *Neurosci. Lett.* **121,** 119–121 (1991).
33. Grynkiewicz, G., Poenie, M. & Tsien, R. Y. *J. biol. Chem.* **260,** 3440–3450 (1985).
34. Connor, J. A. *Cell Calcium* **14,** 173–188 (1993).
35. Connor, J. A. & Nikolakopoulou, G. *Lec. Math. Life Sci.* **15,** 79–101 (1982).
36. Cohan, C. S., Connor, J. A. & Kater, S. B. *J. Neurosci.* **7,** 3588–3599 (1987).
37. McCobb, D. P., Cohan, C. S., Connor, J. A. & Kater, S. B. *Neuron* **1,** 377–385 (1988).
38. Spitzer, C. C. & Lamborghini, H. E. *Proc. natn. Acad. Sci. U.S.A.* **73,** 1641–1645 (1976).
39. Anderson, M. J., Cohen, M. W. & Zorychta, E. *J. Physiol., Lond.* **268,** 731–758 (1977).
40. Tabti, N. & Poo, M-m. in *Culturing Nerve Cells* (eds Banker, G. & Goslin, K.) 137–153 (MIT Press, Cambridge, 1991).

ACKNOWLEDGEMENTS. This work was supported by a grant from the NIH.

Changing subunit composition of heteromeric NMDA receptors during development of rat cortex

Morgan Sheng, Jennifer Cummings, Leslie Ann Roldan, Yuh Nung Jan & Lily Yeh Jan

Howard Hughes Medical Institute and Departments of Physiology and Biochemistry, University of California, San Francisco, California 94143-0724, USA

ACTIVATION of the *N*-methyl-D-aspartate (NMDA) receptor is important for certain forms of activity-dependent synaptic plasticity, such as long-term potentiation (reviewed in ref. 1), and the patterning of connections during development of the visual system (reviewed in refs 2, 3). Several subunits of the NMDA receptor have been cloned: these are NMDAR1 (NR1), and NMDAR2A, 2B, 2C and 2D (NR2A-D)[4–8]. Based on heterologous co-expression studies, it is inferred that NR1 encodes an essential subunit of NMDA receptors and that functional diversity of NMDA receptors *in vivo* is effected by differential incorporation of subunits NR2A–NR2D[5–8]. Little is known, however, about the actual subunit composition or heterogeneity of NMDA receptors in the brain. By co-immunoprecipitation with subunit-specific antibodies, we present here direct evidence that NMDA receptors exist in rat neocortex as heteromeric complexes of considerable heterogeneity, some containing both NR2A and NR2B subunits. A progressive alteration in subunit composition seen postnatally could contribute to NMDA-receptor variation and changing synaptic plasticity during cortical development.

NR1-FP antibodies, which are raised against NR1 fusion proteins and should recognize all known splice forms of the NR1 subunit[9,10], bind to a heterogeneous band of relative molecular mass (M_r) ~120K on immunoblots of rat brain membranes (Fig. 1), in agreement with the reported size of the NR1 protein[11,12]. NR1-C1 and NR1-N1 antibodies, raised against alternatively spliced exons of NR1, recognize distinct, though overlapping, subsets of the bands recognized by NR1-FP, conwith their specificity for different overlapping subsets of splice variants of NR1[9,10]. NR2A and NR2B antibodies recognize bands of M_r ~165K and ~170K, respectively, consistent with predicted sizes of NR2A and NR2B[5–8].

After solubilization of cortical membranes with 'RIPA' buffer (see Fig. 2 legend), NR1-FP, NR1-C1 and NR1-N1 antibodies immunoprecipitate not only NR1 polypeptides, as expected, but also significant amounts of NR2A and NR2B (Fig. 2). Conversely, NR2A and NR2B antibodies immunoprecipitate NR1 proteins in addition to their respective cognate antigens. The mutually consistent results obtained with five independent anti-

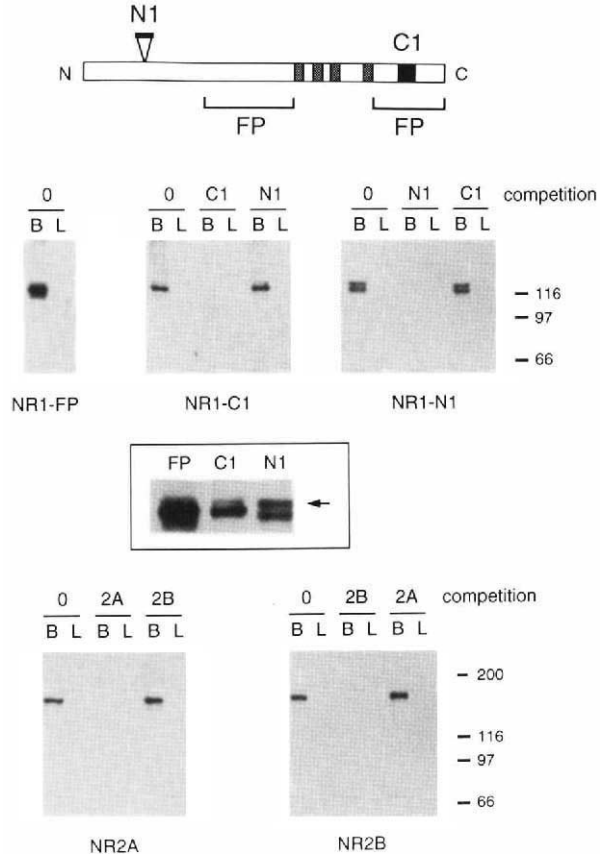

FIG. 1 NMDA-receptor subunit-specific antibodies. Top section: Diagram of the NR1 protein, showing positions of alternatively spliced N1 and C1 exons. Brackets indicate the segments of NR1 incorporated in fusion proteins for raising NR1-FP antibodies. Putative transmembrane segments are shown (stippled). Middle and bottom sections: Immunoblots of membrane proteins from whole rat brain (B) or rat liver (L) were probed with affinity-purified antibodies to NR1-FP, C1, N1, NR2A or NR2B, as indicated at the bottom of each panel. Immunoblots were probed in the absence of competitor (0), or in the presence of various competitor peptides (10 μg ml^{-1}), as indicated. Boxed inset shows in detail the bands recognized by NR1-FP, C1 and N1 antibodies. The doublets recognized by C1- and N1-exon-specific antibodies correspond to different but overlapping subsets of the heterogeneous band(s) recognized by the NR1-FP antibodies. The upper co-migrating band recognized by both C1 and N1 antibodies (arrow) probably contains NR1 polypeptides which incorporate both the C1 and N1 exons (see text).
METHODS. Rabbit antibodies were raised against the following peptides: C1:CDRKSGRAEPDPKKKATFRAITSTLASSFKRRRTSKDT (residues 864–900 of NMDAR1, ref. 4, corresponding to exon 5, ref. 9. N1:SKKRNYENLDQLSYDNKRGPKC, corresponding to exon 21, ref. 9; NR2A:CDNILDKPREIDLSRPSRSISLKDRERLLE (residues 1,293–1,321)[8]; NR2B:SPHWEHVDLTDIYKERSDDFKRDSVSGGGPC (residues 1,143–1,173)[8]. Underlined cysteine residues were added for coupling to carrier. NR1-FP antibodies were raised against two bacterial fusion proteins containing residues 339–561 and 834–938 of NMDAR1 (ref. 4) inserted in-frame in vector pRSETB (Invitrogen), and induced and purified on zinc columns according to the manufacturer's directions. Kv1.4 antibodies have been described[26]. All antibodies were affinity-purified using their respective immunogens coupled to Sulfolink columns (Pierce) or Affi-Gel 10 (Biorad). Immunoblots were performed as described[27].